Article

Cell Chemical Biology

Biosynthesis and Activity of Prenylated FMN Cofactors

Graphical Abstract

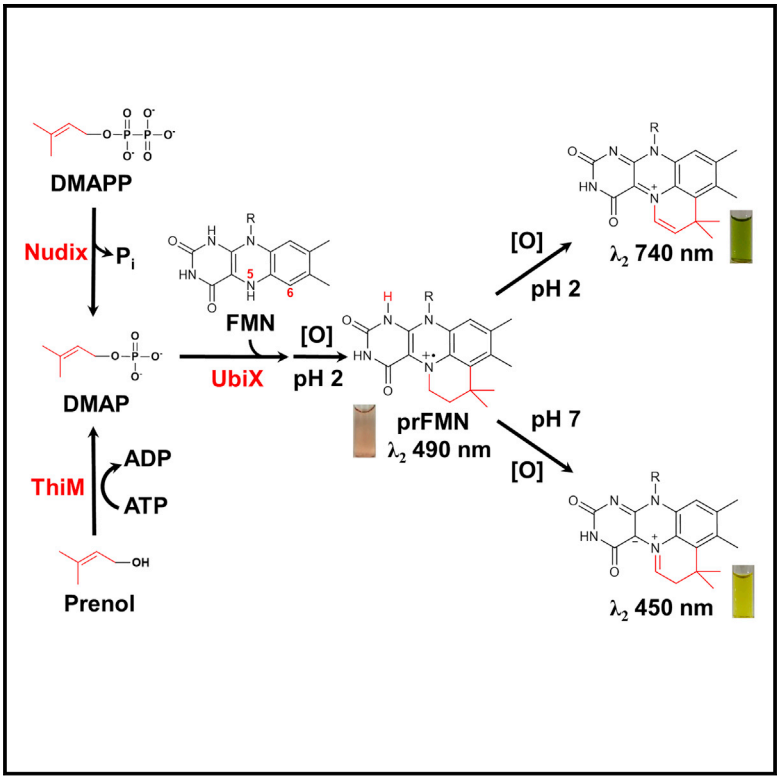

Authors

Po-Hsiang Wang,
Anna N. Khusnutdinova, Fei Luo, ...,
Radhakrishnan Mahadevan,
Elizabeth A. Edwards,
Alexander F. Yakunin

Correspondence

elizabeth.edwards@utoronto.ca (E.A.E.),
a.iakounine@utoronto.ca (A.F.Y.)

In Brief

Wang et al. characterized the biosynthetic origin of the prenyl donor of prenylated FMN in *E. coli*, a newfound cofactor involved in ubiquinone biosynthesis and lignin biodegradation. They developed methods to produce free prenylated FMN species. These findings suggested a novel metabolic link between the isoprenoid pathway and ubiquinone biosynthesis.

Highlights

- FMN prenylation activity is conserved in the UbiX family
- *E. coli* produces DMAP by phosphorylation of prenol and dephosphorylation of DMAPP
- Identification and biochemical characterization of new forms of prFMN
- A novel metabolic link between the isoprenoid pathway and ubiquinone biosynthesis

Wang et al., 2018, Cell Chemical Biology *25*, 1–11
May 17, 2018
https://doi.org/10.1016/j.chembiol.2018.02.007

CellPress

Please cite this article in press as: Wang et al., Biosynthesis and Activity of Prenylated FMN Cofactors, Cell Chemical Biology (2018), https://doi.org/10.1016/j.chembiol.2018.02.007

Cell Chemical Biology
Article

Biosynthesis and Activity of Prenylated FMN Cofactors

Po-Hsiang Wang,[1,3] Anna N. Khusnutdinova,[1,3] Fei Luo,[1] Johnny Xiao,[1] Kayla Nemr,[1] Robert Flick,[1] Greg Brown,[1] Radhakrishnan Mahadevan,[1] Elizabeth A. Edwards,[1,2,*] and Alexander F. Yakunin[1,4,*]
[1]Department of Chemical Engineering and Applied Chemistry, University of Toronto, 200 College Street, Toronto, ON M5S 3E5, Canada
[2]Department of Cell and Systems Biology, University of Toronto, 25 Harbord Street, Toronto, ON M5S 3E5, Canada
[3]These authors contributed equally
[4]Lead Contact
*Correspondence: elizabeth.edwards@utoronto.ca (E.A.E.), a.iakounine@utoronto.ca (A.F.Y.)
https://doi.org/10.1016/j.chembiol.2018.02.007

SUMMARY

Prenylated flavin mononucleotide (prFMN) is a recently discovered cofactor required by the UbiD family of reversible decarboxylases involved in ubiquinone biosynthesis, biological decomposition of lignin, and biotransformation of aromatic compounds. This cofactor is synthesized by UbiX-like prenyltransferases catalyzing the transfer of the dimethylallyl moiety of dimethylallyl-monophosphate (DMAP) to FMN. The origin of DMAP for prFMN biosynthesis and the biochemical properties of free prFMN are unknown. We show that in *Escherichia coli* cells, DMAP can be produced by phosphorylating prenol using ThiM or dephosphorylating DMAPP using Nudix hydrolases. We produced 14 active prenyltransferases whose properties enabled the purification and characterization of protein-free forms of prFMN. *In vitro* assays revealed that the UbiD-like ferulate decarboxylase (Fdc1) can be activated by free prFMN$_{iminium}$ or C2′-hydroxylated prFMN$_{iminium}$ under both oxidized and reduced conditions. These insights into the biosynthesis and properties of prFMN will facilitate further elucidation of the biochemical diversity of reversible UbiD (de) carboxylases.

INTRODUCTION

The enzyme cofactors flavin mononucleotide (FMN) and flavin adenine dinucleotide were discovered more than 80 years ago (Haas, 1938). Flavin-containing enzymes or flavoenzymes account for approximately 1% of cellular proteins and catalyze a plethora of redox reactions with organic substrates (Leys and Scrutton, 2016; Piano et al., 2017; Walsh and Wencewicz, 2013). In addition to catalyzing common redox reactions in cell metabolism, DNA repair, protein folding, and degradation of aromatics, flavoenzymes can catalyze acid/base and nucleophilic/electrophilic reactions (Sobrado, 2012), as well as reactions with mechanisms that involve the formation of highly reactive covalent flavin-substrate intermediates (Teufel et al., 2016).

Some enzymes use modified flavins, including the most recently discovered prenylated FMN (prFMN) cofactor in the active site of the *Aspergillus niger* ferulic acid decarboxylase Fdc1, which is required for the non-oxidative reversible decarboxylation of α,β-unsaturated acids via 1,3-dipolar cycloaddition (Payne et al., 2015). Fdc1 belongs to the widespread family of UbiD-like proteins named after *Escherichia coli* UbiD involved in the biosynthesis of ubiquinone (Cox et al., 1969; Payer et al., 2017). Previous genetic studies suggested that *ubiD* and the associated *ubiX* are isofunctional genes, encoding redundant aromatic decarboxylases (Zhang and Javor, 2003), although decarboxylase activity had not been demonstrated for both proteins (Gulmezian et al., 2007; Jacewicz et al., 2013; Kopec et al., 2011; Rangarajan et al., 2004). A 2015 study with the *Saccharomyces cerevisiae* UbiX-like Pad1 and UbiD-like Fdc1 revealed that rather than being a decarboxylase, Pad1 actually catalyzes the formation of a novel, diffusible FMN-type cofactor required for decarboxylase activity of Fdc1 (Lin et al., 2015). This work also demonstrated that the *S. cerevisiae* Fdc1 can be activated *in vivo* by co-expression with *E. coli* UbiX. The nature of the FMN modification and UbiX activity were determined by structural and biochemical studies of the UbiD from *A. niger*, *S. cerevisiae*, and *Candida dubliniensis*, as well as the UbiX-like PA4019 from *Pseudomonas aeruginosa* (Payne et al., 2015; White et al., 2015). The authors demonstrated that UbiD is responsible for decarboxylase activity, which required a prFMN produced by PA4019.

High-resolution crystal structures of UbiD in complex with oxidized prFMN revealed the presence of at least three cofactor forms: prFMN-N5-iminium (prFMN$_{iminium}$), prFMN ketimine, and C1′-hydroxylated prFMN, and suggested that prFMN$_{iminium}$ represented the catalytically active species (Payne et al., 2015). PA4019 was found to be an FMN prenyltransferase, which transfers a dimethylallyl moiety from dimethylallyl-monophosphate (DMAP) to the flavin N5 and C6 atoms, adding a fourth ring to the FMN isoalloxazine group (Figure 1A). This reaction required the reduction of the FMN-DMAP-PA4019 complex by dithionite (DT) followed by re-oxidation by air, producing a stable purple-colored protein with a second absorbance maximum (λ_2) at 550 nm (White et al., 2015). However, a recent study revealed that, in contrast to bacterial UbiX, the *S. cerevisiae* UbiX-like protein PAD1 prefers dimethylallyl-pyrophosphate (DMAPP) as the prenyl group donor, which is a common precursor in isoprenoid biosynthesis (Arunrattanamook and Marsh, 2017). Liquid

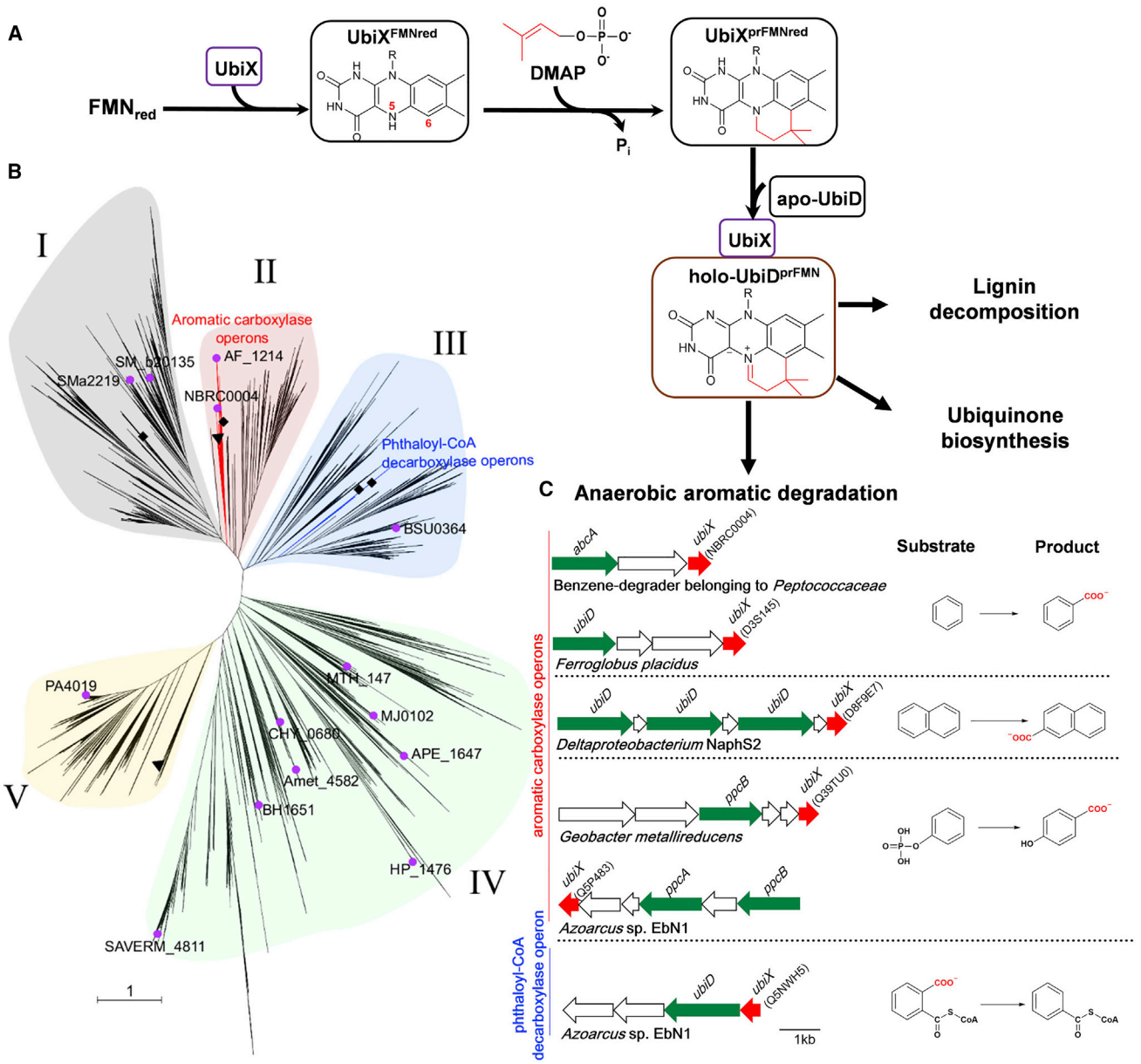

Figure 1. Phylogenetic Analysis of the UbiX Family

(A) Schematic diagram showing UbiX-catalyzed biosynthesis of prFMN and its roles in biological processes.

(B) Unrooted phylogenetic tree of the UbiX family showing five UbiX clusters (I–V). Cluster II includes UbiX sequences from known anaerobic aromatic degradation operons, whereas cluster III contains UbiX genes from the phthaloyl-CoA decarboxylase operons. UbiX paralogs from *Azoarcus* sp. strain EbN1 and *G. metallireducens* are labeled as ◆ and ▼, respectively. UbiX-like proteins purified in this work including PA4019 and AF1214 are marked with purple circles and labeled.

(C) Anaerobic aromatic degradation operons from different organisms containing *ubiX* (red arrows) and *ubiD* (green arrows) genes, as well as their substrates and products.

chromatography-mass spectrometry (LC-MS) analysis of small molecule extracts from both reduced and re-oxidized PA4019 complexes showed the presence of fully reduced prFMN ($prFMN_{red}$) and prFMN-C4a-radical ($prFMN_{radical}$), respectively (White et al., 2015). Decarboxylase activity of the *A. niger* Fdc1 could be reconstituted by anaerobic incubation with PA4019 containing $prFMN_{red}$ ($PA4019^{prFMNred}$), followed by re-oxidation by air, but not with $PA4019^{prFMNradical}$, suggesting that UbiD requires $prFMN_{red}$ to be oxidized to the catalytically active $prFMN_{iminium}$ (Payne et al., 2015). In addition, the Fdc1 reconstitution appeared to be independent of the presence of UbiX, because Fdc1 activity was also observed using protein-free extracts of $PA4019^{prFMNradical}$ (Payne et al., 2015) and holo-Fdc1 (Lin et al., 2015), respectively. The crystal structure of an

Fdc1-prFMN complex (Fdc1^{prFMN}) suggested that the reversible substrate decarboxylation proceeded via 1,3-dipolar cycloaddition of the prFMN$_{iminium}$ azomethine ylide to the α,β-double bond of substrate side chain (Payne et al., 2015), which was also supported by molecular modeling (Tian and Liu, 2017), kinetic isotope effects (Ferguson et al., 2016), and mechanism-based inhibitor analysis (Ferguson et al., 2017).

The remarkable discovery of prFMN structure and associated catalytic mechanism for decarboxylation gives rise to many important questions, including confirmation of FMN prenyltransferase activity in other UbiX-like proteins, the biosynthetic origin of DMAP, as well as the biochemical properties of free prFMN and how these affect interactions with UbiD. In this study, we completed a phylogenetic analysis of over 9,000 UbiX-like proteins and demonstrated FMN prenyltransferase activity in 14 UbiX-like proteins from different phylogenetic groups. We found that in *E. coli,* DMAP can be produced by direct phosphorylation of prenol by the kinase ThiM and by dephosphorylation of DMAPP by the Nudix hydrolases NudF and NudJ. Using optimized reaction conditions, we produced several protein-free prFMN forms, including a red-colored protonated prFMN$_{radical}$, and demonstrated activation of apo-Fdc1 by free cofactors.

RESULTS AND DISCUSSION

Phylogenetic Analysis of the UbiX Family of FMN Prenyltransferases

Most of the over 9,000 UbiX-like sequences (IPR004507, InterPro database) are present in bacterial genomes (>7,800 genes) with the remaining sequences found in archaea (~500 genes), fungi, and unicellular algae (>500 genes). Phylogenetic analysis of the UbiX family revealed the presence of at least five major clusters (I–V) (Figures 1B and S1). Some bacterial genomes contain more than one *ubiX* gene, in which case these genes are typically found in separate operons, suggesting involvement in different anabolic or catabolic processes. For example, there are two distinct *ubiX* genes in *Geobacter metallireducens* and four in *Azoarcus* sp. EbN1 (*Aromatoleum aromaticum* EbN1). In *G. metallireducens,* the *ubiX* gene in the phenyl-phosphate carboxylase operon (Q39TU0, Gmet2105) encodes a protein that clusters with UbiX sub-family II, whereas the second *ubiX* gene (Q39Q70, Gmet3392, 38% sequence identity to Gmet2105) encodes a protein that clusters with UbiX sub-family V (Figure 1B). Of the four *ubiX* paralogs in *Azoarcus* sp. strain EbN1, one (Q5P483) is in the phenyl-phosphate carboxylase operon, two (D5NWH5 and D5NWG7) are in the phthaloyl-CoA decarboxylase operon, and the fourth (Q5P010) appears to be a single gene (Table S1), and each encodes proteins that cluster with different UbiX sub-families (I, II, and III) (Figure 1B). UbiX, whose genes are co-operonic with *ubiD* genes encoding (de) carboxylases involved in the degradation of aromatic compounds (benzene, phthalate, phenol, or naphthalene), are located in UbiX sub-families II (aromatic carboxylase operons) and III (phthaloyl-CoA decarboxylase operons) (Figures 1B and 1C; Table S1). Finding multiple *ubiX* genes within a single genome with different phylogenies suggests that some may have been horizontally acquired.

Purification of Novel UbiX-like Proteins with Bound prFMN

We cloned 23 UbiX-like proteins sampled around the phylogenetic tree for recombinant expression in *E. coli* BL21 (Figures 1B and S2). Preliminary expression experiments with the recently characterized PA4019 revealed that aerobically grown *E. coli* cultures produced colorless PA4019, whereas a purple-colored protein was purified from cultures that were rendered anaerobic after induction with isopropyl-β-D-1-thiogalactopyranoside (IPTG) and that were also provided with riboflavin (FMN precursor) and prenol, a possible DMAP precursor (Figures 2A and S3A). These results suggested that prFMN biosynthesis in *E. coli* cells might be limited by low intracellular concentrations of DMAP. When the 23 cloned UbiX-like proteins were over-expressed using this optimized protocol (anaerobic conditions with the addition of riboflavin and prenol), we were able to purify 14 soluble proteins, of which five showed purple color in the preparations: AF1214 from *Archaeoglobus fulgidus*, MJ0101 from *Methanocaldococcus jannaschii*, SMb20135 from *Sinorhizobium meliloti*, MTH0147 from *Methanothermobacter thermoautotrophicus*, and PA4019 (Table S2). Absorption spectra confirmed the presence of prFMN$_{radical}$ (λ_1 360 nm and λ_2 550 nm) in these preparations (data not shown). Additional expression trials with AF1214 revealed that, in contrast to PA4019, the AF1214 preparations purified from either aerobically or anaerobically grown cultures without prenol addition had yellow color with absorption spectra typical of FMN-containing proteins with λ_1 at 370 nm and λ_2 at 460 nm (Figure 2B, samples I, II, and VI). Aerobic preparations with prenol addition also showed similar spectra (Figure 2B, sample IV). However, anaerobic expression of AF1214 in the presence of prenol produced purple-colored preparations with absorption spectra, indicating the presence of prFMN$_{radical}$ with λ_1 at 360 nm and λ_2 at 550 nm (Figure 2B, samples VII and VIII). The addition of riboflavin to these cultures did not alter the results. Therefore, recombinant expression of AF1214^{prFMN} in *E. coli* seemed to be limited by intracellular DMAP levels, and this limitation could be overcome by the addition of prenol to the growth medium. In addition, AF1214 appeared to have a higher affinity to FMN compared with PA4019, as the former retained FMN even after protein purification from aerobically grown *E. coli* cultures.

In Vitro Prenylation of FMN by PA4019 and AF1214

PA4019 was shown to bind free FMN in the presence of DMAP, but for FMN prenylation, this complex required reduction by DT followed by re-oxidation by air to produce a stable purple-colored prFMN$_{radical}$ (White et al., 2015). We found that FMN binding by the colorless (FMN-free) AF1214 (Figure 2B; sample V) under anaerobic conditions (reduced by DT) was stimulated by the addition of orthophosphate alone, and was further stimulated by addition of DMAP (Figure S4A). Interestingly, both orthophosphate and DMAP showed no stimulation of FMN binding by AF1214 under aerobic conditions (Figure S4B). Furthermore, reduction of AF1214^{FMN} (samples I and II in Figure 2B) by DT in the presence of DMAP followed by air oxidation resulted in FMN prenylation and formation of purple-colored AF1214^{prFMNradical} based on absorption spectrum (Figure S4C). Substrate saturation experiments with DMAP revealed that FMN prenylation by AF1214^{FMN} is saturated with 100 μM

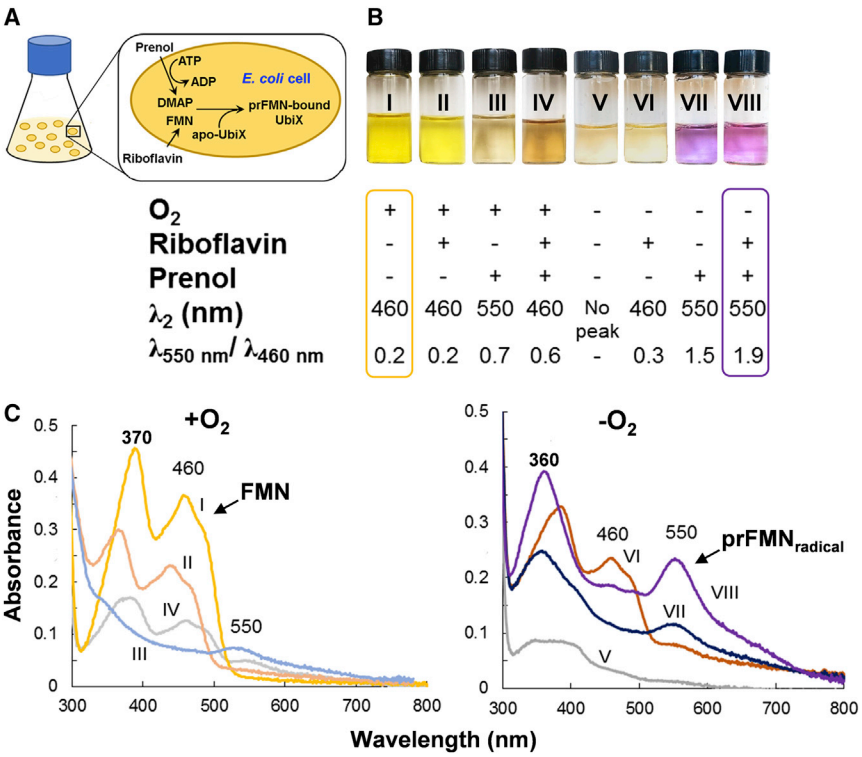

Figure 2. Recombinant Expression and Purification of the UbiX-like AF1214

(A) Schematic diagram showing UbiX expression experiment in *E. coli* cultures.

(B) Vials of AF1214 preparations purified from *E. coli* cells grown under different conditions as indicated. The results ($\lambda_{550}/\lambda_{460}$) show the mean ± SEM from independent experiments performed at least in duplicate (variation ~20%).

(C) Absorption spectra of purified AF1214 (depicted in B).

DMAP with apparent K_m 30 μM (Figure S4D). Thus, AF1214 ^{FMN} can be used as an indicator protein for DMAP detection based on changes in absorption spectrum following DT reduction and air oxidation. Optimized conditions for *in vitro* FMN prenylation by UbiX (orthophosphate added) enabled the assay of the 14 previously purified soluble UbiX-like proteins for FMN prenylation activity. We detected purple color in the preparations of HP1451 from *Helicobacter pylori* and JGI0011 from *Alkaliphilus metalliredigens*, indicating formation of $prFMN_{radical}$ that was retained within the enzyme (Table S2). For the remaining proteins, LC-MS analysis of protein-free reaction filtrates confirmed production of $prFMN_{iminium}$ and prFMN-OH by all purified colorless UbiX-like proteins (Figure S4E), including NBRC0004 from a benzene-degrading *Peptococcaceae* sp. (Figure 1C; Table S2). This suggests that prFMN is likely involved in the predicted benzene carboxylation reaction catalyzed by the associated putative UbiD-like anaerobic benzene carboxylase, AbcA (Figure 1C). While all purified UbiX-like proteins tested possess FMN prenylation activity, they seem to have different affinities to the reaction product, prFMN (Figure S4E). Nevertheless, FMN prenylation activity appears to be conserved in all major phylogenetic groups of the UbiX family.

Biosynthesis of DMAP in *E. coli* Cells: Prenol and DMAPP as Precursors

We sought to investigate the origin of DMAP required by UbiX for prFMN biosynthesis. Partially purified *E. coli* cell lysates were reported to phosphorylate prenol to DMAP (Lange and Croteau, 1999), which was confirmed in the experiments using *E. coli* BL21 wild-type cell lysates in the presence of ATP and Mg^{2+} (Figure S3B). This is consistent with our finding that prenol addition to *E. coli* cultures stimulated the formation of prFMN by recombinant UbiX-like proteins (Figures 2B and S3A). To identify *E. coli* kinases that can phosphorylate prenol to DMAP, we used the purified AF1214^{FMN} as a reporter protein to screen *E. coli* cell lysates overexpressing 98 *E. coli* kinases known to be active toward hydroxyl-containing substrates, as well as several uncharacterized kinases (Table S3). As shown in Figure 3A, after IPTG induction of kinase expression, the cell lysates were prepared and incubated for 1 hr with prenol, ATP, and purified AF1214^{FMN} (yellow), followed by FMN reduction by DT and re-oxidation by air (Figure 3A). Of the 98 clones screened, at least 16 lysates developed a weak reddish color (Table S4A), which correlated with higher values of the $\lambda_{550\ nm}/\lambda_{460\ nm}$ ratio (0.2–1.0), suggesting the formation of AF1214^{prFMNradical}. The recombinant proteins from the positive clones were affinity purified, and a second AF1214-based screen confirmed the presence of prenol kinase activity in the hydroxyethylthiazole kinase ThiM (Figure 3B). ThiM, a salvage enzyme in thiamine biosynthesis, has been shown to catalyze the phosphorylation of 4-methyl-5-beta-hydroxyethylthiazole (THZ) (Mizote and Nakayama, 1989), with structural similarity to prenol (Figure S5A). Alanine replacement mutagenesis confirmed that the prenol kinase activity of ThiM depended on the residues known to be critical for THZ phosphorylation (Figure S5B) (Dyguda-Kazimierowicz et al., 2007). Prenol addition to *E. coli* BL21 wild-type cultures had no measurable effect on ThiM protein expression level based on LC-MS analysis (Tables S4B and S5), whereas a small decrease in activity in the *thiM* deletion (Δ*thiM::Cm*^{R}) strain was observed using the PA4019-based assays for prFMN formation, suggesting that additional proteins in *E. coli* have prenol kinase activity (Figure S5C). In the presence of ATP and Mg^{2+}, purified ThiM catalyzed comparable phosphorylation rates both with prenol and THZ (0.18 and 0.19 μmol/min/mg protein, respectively), but had lower affinity for prenol (K_m 14 mM) compared with THZ (K_m 2.0 mM) (Figure S5A).

Another possible biosynthetic route to DMAP in bacteria is from DMAPP dephosphorylation. DMAPP is an intermediate in the mevalonate (Meganathan, 2001) or MEP (2-C-methyl-D-erythritol 4-phosphate) (Lichtenthaler et al., 1997) isoprenoid biosynthesis pathways. Our preliminary results indicated that Mg^{2+} addition stimulated DMAPP and DMAP dephosphorylation in *E. coli* cell extracts (Figures 3C and 3D). In addition, *E. coli*

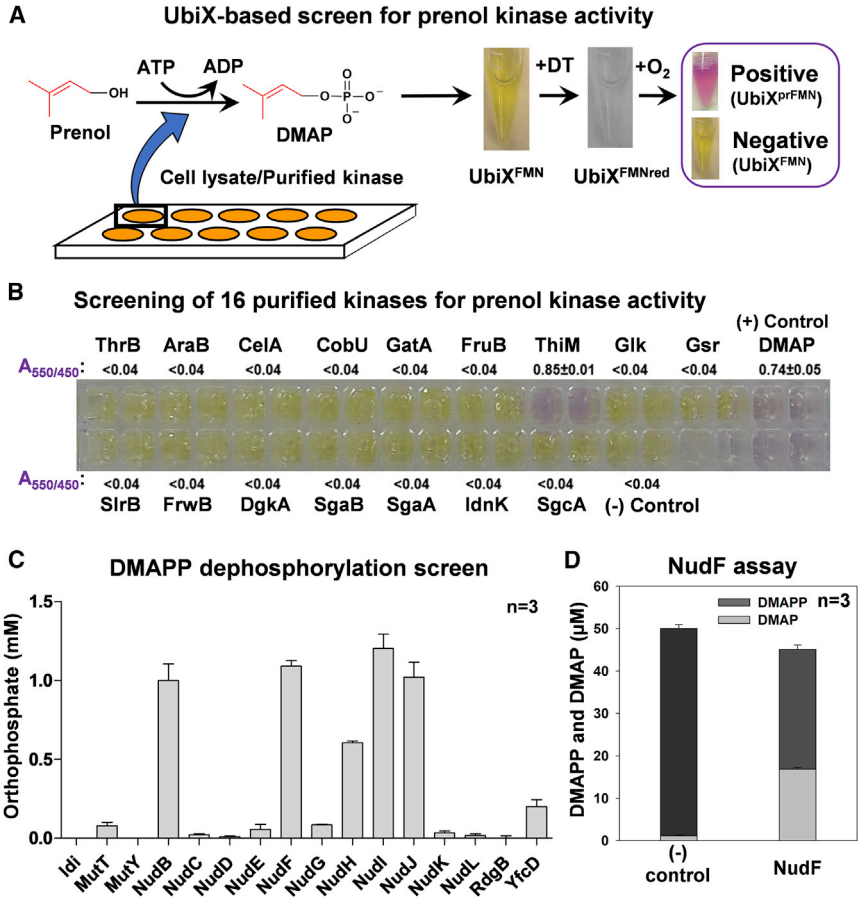

Figure 3. Screening for DMAP-producing Enzymes

(A) Schematic diagram showing the AF1214-based screen for prenol kinase activity using *E. coli* cell lysates (first round), or purified candidate proteins (second round, shown in B).

(B) Microplate wells showing the results of AF1214-based screening (second round) of 16 purified candidate proteins. The purple color of two wells with ThiM suggests the presence of prenol kinase activity in this protein. DMAP: a positive control with 1 mM DMAP added instead of protein. $\lambda_{550\ nm/450\ nm}$: the ratio (multiplied by 10) of reaction mixture absorbance at 550 nm–450 nm indicating the formation of prFMN (from the produced DMAP).

(C) Screening of 16 purified *E. coli* phosphohydrolases for DMAPP dephosphorylation activity. Production of orthophosphate after incubation of DMAPP (1 mM) with 16 purified *E. coli* Nudix hydrolases.

(D) LC-MS analysis of DMAPP conversion to DMAP by the *E. coli* NudF.

Values represent means ± SEM from independent experiments in duplicate for (B) and in triplicate for (C) and (D).

cultures over-expressing the Nudix hydrolase NudF (ADP-ribose pyrophosphatase) were reported to dephosphorylate DMAPP to prenol (Zheng et al., 2013). However, the intermediary products of DMAPP dephosphorylation by purified Nudix enzymes have not yet been analyzed. Therefore, we screened 16 purified *E. coli* Nudix hydrolases and nucleotide pyrophosphatase RdgB (YggV; Table S3) for DMAPP dephosphorylation. These screens revealed high DMAPP dephosphorylation activity in four Nudix proteins, including NudB, NudF, NudI, and NudJ, which completely hydrolyzed 1 mM DMAPP after 20 min incubation (Figure 3C). LC-MS analysis of NudF reaction mixtures revealed the presence of DMAP as the only organic reaction product (prenol undetected) (Figure 3D). Furthermore, LC-MS analysis of the *E. coli* BL21 wild-type proteomes showed significant expression levels of NudF and NudJ, whereas the other two Nudix hydrolases were not detected (Tables S4B and S5). *E. coli* NudJ has been shown to dephosphorylate several nucleoside tri- and di-phosphates and thiamine pyrophosphate to corresponding monophosphate products (Lawhorn et al., 2004; Xu et al., 2006). DMAPP saturation experiments with purified NudF and NudJ revealed similar K_m values (0.8 mM and 0.5 mM, respectively), but NudJ had two times higher V_{max} (0.3 μmol/min/mg protein) than NudF (0.15 μmol/min/mg protein) (Figures S5D and S5E). With GDP and ADP-ribose as substrates, these enzymes have been reported to have similar K_m values (0.6 mM and 0.1 mM, respectively), but higher V_{max} (12–297 μmol/min/mg protein) (Dunn et al., 1999; Xu et al., 2006). Nevertheless, DMAPP dephosphorylation assays with cell lysates from *E. coli* cells with singly or doubly deleted genes (Δ*nudJ::Km*^{R}; Δ*nudF::Km*^{R}; or Δ*nudJ::Km*^{R}, Δ*nudF::Cm*^{R}) indicated that both enzymes can contribute to the *in vivo* production of DMAP from DMAPP (Figure S5F). Thus, our results suggest that in *E. coli* cells, ThiM can produce DMAP via prenol phosphorylation, whereas NudF and NudJ can dephosphorylate DMAPP to DMAP.

Extraction and Biochemical Characterization of Free prFMN Forms

High-temperature extraction of PA4019^{prFMNradical} in 70% acetonitrile under anaerobic conditions and neutral pH released purple-colored prFMN$_{radical}$, identified by MS as an [M-H]$^-$● adduct with *m/z* = 524.165 in negative-ion mode (form B_2 in Figures 4A and S6A). However, high-temperature extraction of AF1214^{prFMNradical} under neutral pH did not release free prFMN, likely due to protein thermostability. UV-vis absorption spectrum of free prFMN$_{radical}$ (B_2) was similar to that of the UbiX-bound prFMN$_{radical}$ (B_1), but its λ_2 shifted to 515 nm (Figure 4B*i*), whereas air exposure resulted in rapid loss of purple color and peak disappearance. This is in contrast to the protein-bound prFMN$_{radical}$ (B_1), which was found to be stable under aerobic conditions, suggesting that UbiX protects prFMN from O_2.

The addition of 50–100 mM HCl to free prFMN$_{radical}$ (B_2) under anaerobic conditions changed its color from purple to red, and the absorption spectrum showed a shift in the λ_2 peak from 515 nm to 490 nm (Figure 4B*i*). MS analysis of this preparation in positive-ion mode revealed a radical cation (M$^+$●) with *m/z* = 526.182 (Figure 4C*i*). This peak was interpreted as a molecular

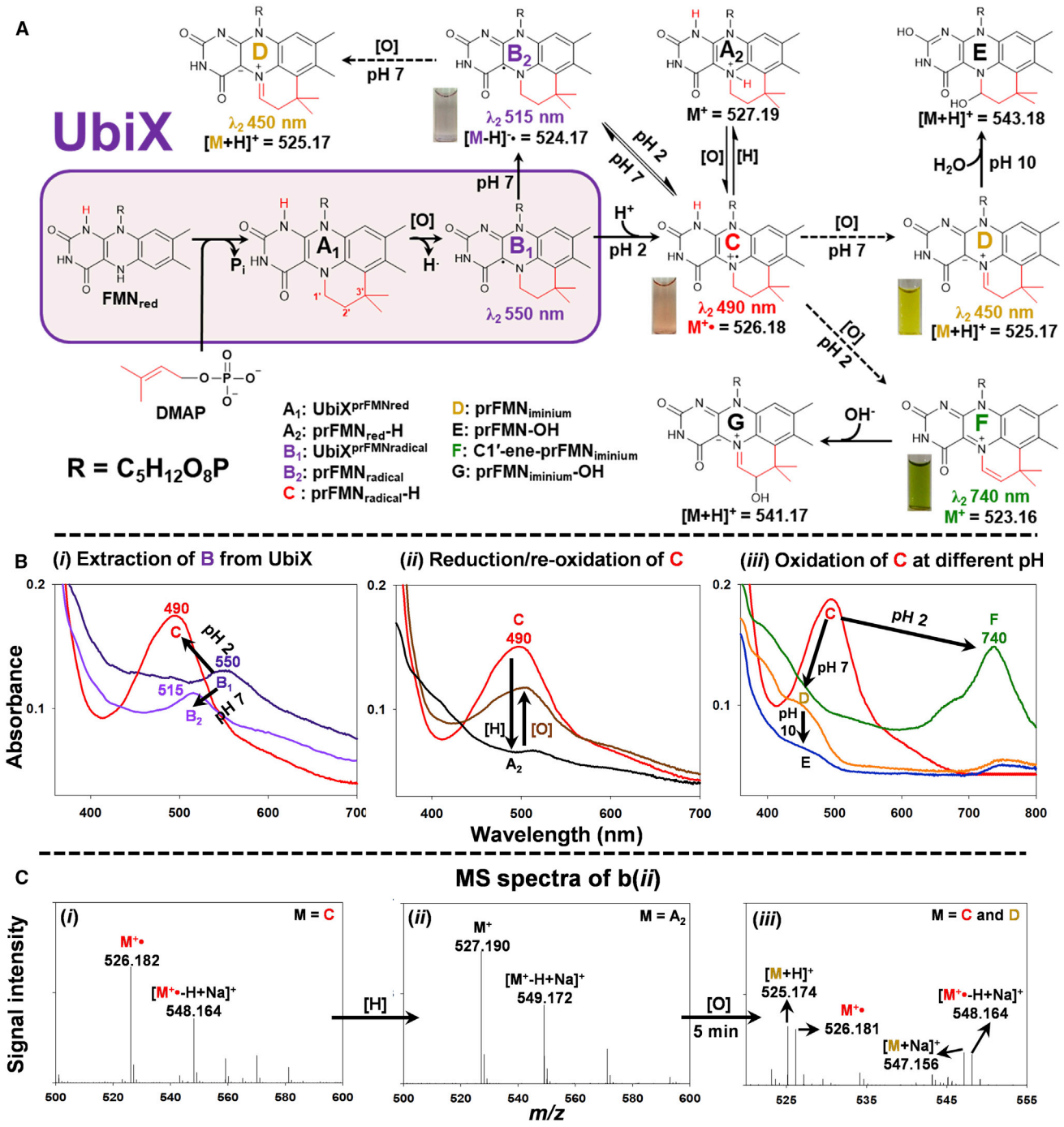

Figure 4. Proposed Biochemical and Chemical Transformations of prFMN

(A) Diagram showing the bioformation of prFMN by UbiX (inside the pale purplish rectangle) and its chemical transformations to other prFMN forms after cofactor extraction and different treatments (acid/alkaline; [H], reduction by DT; [O], oxidation by air). The prFMN forms are labeled as follows: A_1, UbiX-bound $prFMN_{red}$; A_2, protonated $prFMN_{red}$; B_1, UbiX-bound $prFMN_{radical}$; B_2, $prFMN_{radical}$; C, protonated $prFMN_{radical}$; D, $prFMN_{iminium}$; E, C1′-hydroxylated prFMN; F, C1′-ene-$prFMN_{iminium}$; G, C2′-hydroxylated $prFMN_{iminium}$. For free cofactors, the monoisotopic mass is indicated below their structures, as well as the λ_2 peaks and solution color for colored species.

(B) Changes in absorption spectra (λ_2 peaks) of the UbiX-bound $prFMN_{radical}$ form (form B_1) and protonated $prFMN_{radical}$ (form C) to other species: (i) after extraction from UbiX (pH 2 or 7); (ii) after reduction by DT and re-oxidation by air; (iii) after overnight oxidation at different pH at 4°C.

(C) MS spectra of form C after (i) extraction from UibX, followed by (ii) reduction by DT and (iii) re-oxidation by air for 5 min.

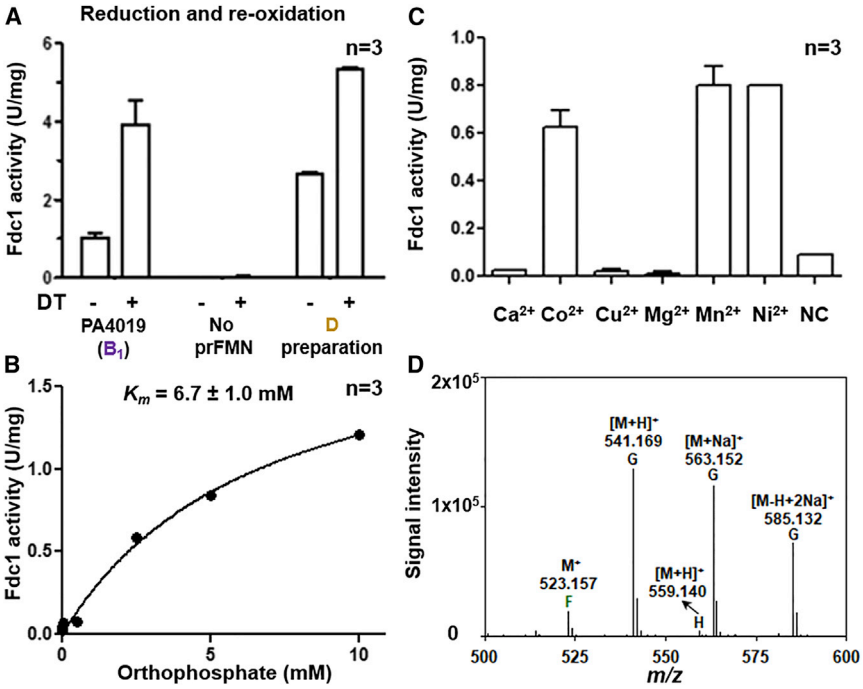

Figure 5. Activation of Fdc1 by UbiX-bound or Protein-free prFMN

(A–C) (A) Fdc1 activity after short incubation with dithionite (DT; 5 min) and the indicated prFMN forms followed by air oxidation and decarboxylation assay with cinnamic acid as substrate; (B) effect of orthophosphate on Fdc1 activation by $prFMN_{iminium}$ followed by decarboxylation assay with cinnamic acid as substrate; (C) effect of divalent metal cations (0.2 mM) on Fdc1 activation by $prFMN_{iminium}$ and decarboxylation activity against cinnamic acid. Values represent means ± SEM from independent experiments in triplicate. (D) Direct-injection MS spectrum of prFMN cofactor extracted from Fdc1 activated by the green-colored F preparation. Abbreviation for prFMN forms: B_1, PA4019-bound $prFMN_{radical}$; D, $prFMN_{iminium}$; F, C1′-ene-$prFMN_{iminium}$; G, C2′-hydroxylated-$prFMN_{iminium}$; H, C1′,C2′-dihydroxylated prFMN.

cation and not the $[M + H]^+$ adduct as the corresponding anionic adduct ($[M-H]^-$) was not observed in negative-ion mode (Schäfer et al., 2007). This suggests the formation of protonated $prFMN_{radical}$ cation at low pH (C in Figure 4A). Furthermore, C was also obtained from $AF1214^{prFMNradical}$ by acidic extraction (50–100 mM HCl) under anaerobic conditions. To determine the extinction coefficient of free prFMN, we used purified $AF1214^{FMN}$. Half of this sample was used to extract FMN and determine its concentration and extinction coefficient (10.9 mM^{-1} cm^{-1}, $\lambda_{442\ nm}$) using a calibration curve prepared with synthetic FMN. The other half was incubated anaerobically with an excess (6x) of DMAP for complete transformation of FMN to prFMN (confirmed by LC-MS analysis; Figure S7A), and subsequent cofactor extraction. Based on the absorbance of purified prFMN samples at 490 nm (λ_2) and assuming all FMN was converted to prFMN, we calculated the extinction coefficient of protonated $prFMN_{radical}$ (C) to be 6.3 mM^{-1} cm^{-1} at $\lambda_{490\ nm}$ (Figure S7B).

Protonated $prFMN_{radical}$ (C) reduction by DT resulted in discoloration and disappearance of the $\lambda_{490\ nm}$ peak (Figure 4B*ii*), whereas MS analysis of the reduced sample revealed an M^+ cation with *m/z* = 527.190 (Figure 4C*ii*) corresponding to the monoisotopic mass of the protonated $prFMN_{red}$ cation (A_2 in Figure 4A). The $\lambda_{490\ nm}$ peak of the reduced preparation was partially restored by air oxidation for 1 min (Figure 4B*ii*), suggesting that C and A_2 can undergo reversible reduction and oxidation. Air exposure of the partially oxidized preparation for an additional 5 min caused a significant decrease in $\lambda_{490\ nm}$ with a color change from red to yellow. MS analysis of this sample revealed the presence of a mixture of a M^+ cation and $[M + H]^+$ adduct with *m/z* = 526.182 and 525.174 (Figure 4C*iii*) corresponding to monoisotopic masses of protonated $prFMN_{radical}$ (C) and $prFMN_{iminium}$ (D in Figure 4A), respectively. After overnight air exposure of C at neutral pH (7), most of this cofactor was oxidized to D, which has been identified as the catalytically relevant prFMN species for Fdc1 (Payne et al., 2015). We found D to be relatively stable under aerobic conditions at neutral pH following overnight incubation at 4°C (retention time 10.5 min in LC-MS; Figure S6C).

Overnight incubation of D at alkaline pH (10) resulted in sample discoloration (Figure 4B*iii*), and LC-MS analysis identified a major $[M + H]^+$ adduct with retention time 10.0 min and *m/z* = 543.18, corresponding to the monoisotopic mass of a C1′-hydroxylated prFMN (E in Figures 4A, 4B*iii*, and S6D). Recently, this form was observed in old crystals of the *A. niger* holo-Fdc1 and acetonitrile extracts of holo-UbiD (Marshall et al., 2017; Payne et al., 2015). However, overnight incubation of C at acidic pH (2) produced a green-colored preparation with λ_2 at 740 nm (Figure 4B*iii*). Adjustment of pH (from 2 to 6) resulted in discoloration of the preparation, and a λ_2 shift from 740 nm to 760 nm. A photodiode array LC-MS analysis assigned the $\lambda_{760\ nm}$ peak at retention time 10.1 min to an M^+ cation with *m/z* = 523.160 (Figures S6B, S6E, and S6F), representing the monoisotopic mass of C1′-ene-$prFMN_{iminium}$ cation (F in Figure 4A). This is consistent with low solubility of F in acetonitrile and its high solubility in water, as well as with the long wavelength absorbance peak at 740 nm due to the presence of a highly conjugated π-system. This form appears to be the product of D oxidation with the loss of a C2′-hydride; however, we found that F can only be produced from C but not from D, suggesting participation of the radical in the acidic oxidation process. Prolonged (2–3 days) storage of either D or F under aerobic conditions resulted in further oxidation of these cofactors. MS analysis of the prFMN extract revealed the presence of two $[M + H]^+$ adducts with *m/z* = 541.17 and 559.18, corresponding to monoisotopic masses of C2′-hydroxylated $prFMN_{iminium}$ (G in Figure 4A) and C1′,C2′-dihydroxylated prFMN forms, respectively (H in Figure S6H). Thus, using purified free prFMN, we confirmed formation of B_2, D, E, F, and G, and proposed two previously unreported forms: C and H (Table S6).

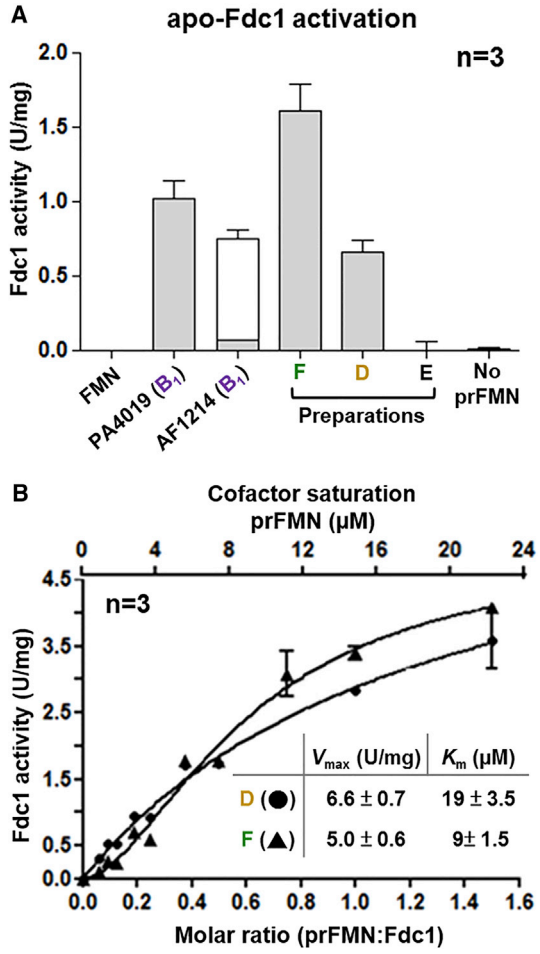

Figure 6. Fdc1 Activation by UbiX-bound and Free prFMN Cofactors

(A) Decarboxylase activity of Fdc1 after 5 min (gray bars) or 60 min (white bar) incubation with a 4 times molar excess of UbiX-bound (PA4019 or AF1214) or free prFMN forms under aerobic conditions (without DT reduction). Free prFMN forms were produced by overnight aerobic incubation of C at 4°C and at different pH (F, D, and E are the major components of the free prFMN preparations at pH 2, pH 7, and pH 10, respectively).

(B) Saturation of purified apo-Fdc1 by the D and F preparations, respectively. The upper x axis shows prFMN concentrations, calculated in respect to the original concentration of C in the preparation prior to oxidation, whereas the lower x axis indicates the prFMN-Fdc1 molar ratio. Values represent means ± SEM from independent experiments in triplicate. Apparent kinetic parameters (K_m and V_{max}) for both preparations are also shown on the graph (R^2 = 0.94 and 0.96, respectively).

In Vitro Activation of Fdc1 Decarboxylase by Free prFMN Forms

The inactive apo-Fdc1 has been shown to be readily activated by *in vitro* anaerobic reconstitution with PA4019^{prFMNred} followed by aerobic oxidation. Decarboxylation activity of the reconstituted holo-Fdc1 was observed only after exposure to air, suggesting that prFMN$_{iminium}$ (D) is the active form of this cofactor (Payne et al., 2015). Since we were able to produce several protein-free prFMN species, we sought to compare them in the Fdc1 activation reaction, as well as to determine the affinity of Fdc1 to free prFMN. First, we observed that purified apo-Fdc1 could be activated in the presence of PA4019^{prFMNradical} (B_1) or by D preparation (prFMN$_{iminium}$ enriched) following DT reduction and air oxidation (Figure 5A). After 5 min activation, Fdc1 activity was ~25% higher in the presence of the free prFMN cofactor. Surprisingly, we found that Fdc1 was also activated by prFMN forms PA4019^{prFMNradical} (B_1) or D under aerobic conditions without DT reduction (Figure 5A). The observed Fdc1 activity without DT reduction was significant (1–2.5 U/mg), although it was 2–3 times lower than that after activation following DT reduction. This suggests that Fdc1 can also bind oxidized prFMN cofactors but appears to have higher affinity to prFMN$_{red}$. Fdc1 activation under aerobic conditions (without DT reduction) was stimulated by addition of orthophosphate (apparent K_m 6.7 ± 1.1 mM) and divalent metal cations (Mn^{2+}, Ni^{2+}, or Co^{2+}) (Figures 5B and 5C). Fdc1 activation by AF1214^{prFMNradical} required longer incubation time likely due to higher affinity of AF1214 to prFMN, but after 60 min activation, Fdc1 showed activity comparable to that obtained with PA4019^{prFMNradical} or D preparation (Figure 6A).

With protein-free prFMN, Fdc1 was activated under aerobic conditions by addition of D preparation and the preparation enriched with C1′-ene-prFMN$_{iminium}$ (F preparation), whereas the preparation enriched with C1′-hydroxylated prFMN (E) and FMN showed no activation (Figure 6A). In these Fdc1 activation experiments, F preparation appeared to be more efficient than D preparation. Cofactor saturation experiments revealed that Fdc1 is saturated by micromolar concentrations of D or F preparations with apparent K_m values 9–19 μM, indicating high affinity of this enzyme to both free species (Figure 6B). Moreover, Fdc1 activated by D or F preparations showed different ratios of decarboxylation activities against cinnamic and α-fluorocinnamic acids (2 and 4, respectively), suggesting that different cofactors (D and F) were involved in these reactions (Table S7). However, it appears that F has no azomethine ylide required to catalyze the 1,3-dipolar cycloaddition (Figure 4A). Therefore, we performed LC-MS analysis of the cofactor extracted under strictly anaerobic conditions from Fdc1 activated by the F preparation. These experiments revealed a significant $[M + H]^+$ adduct with m/z = 541.17 (Figure 5D), corresponding to the monoisotopic mass of C2′-hydroxylated prFMN$_{iminium}$ (form G), which possesses azomethine ylide (Figure 4A). Moreover, this prFMN extract also activated apo-Fdc1 (0.1–0.15 U/mg), suggesting that G is likely the functional prFMN form in the F preparation and may also contribute to bacterial ubiquinone biosynthesis (Figure 7). However, the exact molecular structure of G remains to be confirmed. Thus, our results reveal that apo-Fdc1 can be activated by addition of free prFMN cofactors with or without reduction by DT.

SIGNIFICANCE

UbiX-like proteins from all major phylogenetic groups possess FMN prenylation activity, but exhibit different affinity to prFMN, with some proteins retaining this cofactor after formation. Using optimized reaction conditions for FMN prenylation, we produced protein-free prFMN and proposed two new species: protonated prFMN$_{radical}$ (C) and C1′,C2′-dihydroxylated prFMN (H). Fdc1 activation assays with UbiX-bound and free prFMN showed significant

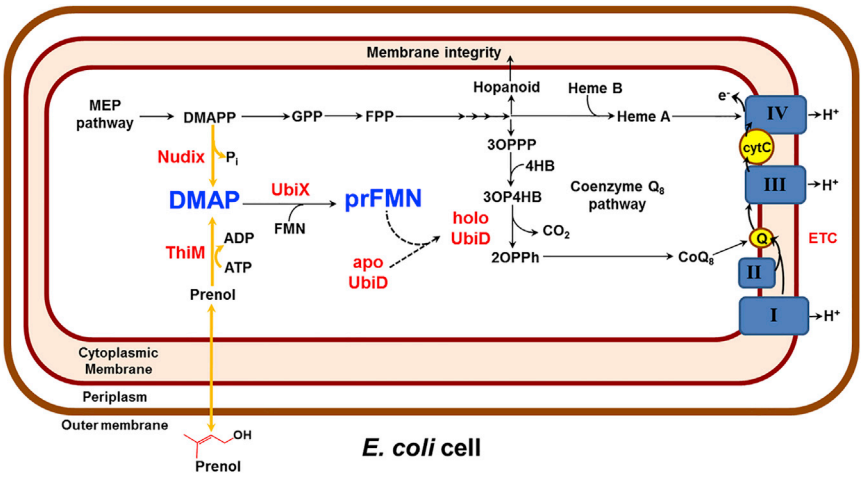

Figure 7. Schematic Overview of the *E. coli* Enzymes Involved in prFMN Biosynthesis and Associated Pathways

Biosynthetic enzymes are shown in red. The novel link between the *E. coli* isoprenoid (MEP) pathway and prFMN biosynthesis is shown by yellow arrows. Chemicals and enzymes involved in the reactions are listed below: Q or CoQ_8, ubiquinone; cyt C, cytochrome C; DMA, dimethylallyl alcohol; DMAP, dimethylallyl-monophosphate; DMAPP, dimethylallyl-pyrophosphate; FMN, flavin mononucleotide; FPP, farnesyl-pyrophosphate; GPP, geranyl-pyrophosphate; 4HB, 4-hydroxybenzoate; 2OPPh, 2-octaprenyl-phenol; 3OP-PP, 3-octaprenyl-pyrophosphate; 3OP4HB, 3-octaprenyl-4-hydroxybenzoate; UbiD, 3-octaprenyl-4-hydroxybenzoate decarboxylase; UbiX, FMN prenyltransferase; prFMN, prenylated-flavin mononucleotide; ThiM, hydroxyethylthiazole kinase; Components of the electron transport chain (ETC): I, NADH dehydrogenase; II, succinate dehydrogenase; III, cytochrome C reductase; IV, cytochrome C oxidase.

enzyme activation under aerobic conditions (without reduction by DT), but anaerobic activation resulted in higher Fdc1 activity. These experiments also revealed a high affinity of Fdc1 to prFMN cofactors, with full enzyme saturation observed at micromolar cofactor concentrations. We found that recombinant expression of $UbiX^{prFMN}$ is stimulated by the addition of prenol to *E. coli* cultures, suggesting that prFMN biosynthesis is limited by intracellular DMAP. Our screens have shown that in *E. coli* cells, DMAP can be produced by direct phosphorylation of added prenol by the ThiM kinase, and by dephosphorylation of DMAPP by the Nudix hydrolases NudJ and NudF. Therefore, the biosynthesis of prFMN from DMAPP provides an additional metabolic link between the UbiX-UbiD pair and isoprenoid biosynthesis pathways, which were already connected through the UbiD-mediated decarboxylation of 3-octaprenyl-4-hydroxybenzoate in ubiquinone biosynthesis (Figure 7). Future studies on prFMN biosynthesis and prFMN-dependent enzymes will likely reveal additional biological roles for this novel cofactor.

STAR★METHODS

Detailed methods are provided in the online version of this paper and include the following:

SUPPLEMENTAL INFORMATION

Supplemental Information includes seven figures and seven tables and can be found with this article online at https://doi.org/10.1016/j.chembiol.2018.02.007.

ACKNOWLEDGMENTS

We thank Dr. David Leys (University of Manchester) and Dr. Alexei Savchenko (University of Toronto) for providing the *A. niger* Fdc1 and UbiX expression plasmids, respectively. This work was supported by the NSERC Industrial Biocatalysis Strategic Network grant and Genome Canada (by the Government of Canada through Genome Canada and the Ontario Genomics Institute, 2009-OGI-ABC-1405). We also acknowledge the help from the BioZone Mass Spectrometry facility (University of Toronto, Canada) for LC-MS analyses.

AUTHOR CONTRIBUTIONS

A.F.Y., E.A.E., and P.H.W. conceptualized this study. A.N.K. and F. L. performed the phylogenetic analysis. A.N.K. and P.H.W. performed enzymatic assays and cofactor characterization. F.L. and J.X. performed proteomic analysis. P.H.W. and R.F. performed LC-MS analyses. K.N. and G.B. performed gene inactivation and site-directed mutagenesis, respectively. A.F.Y., A.N.K., E.A.E., P.H.W., and R.M. wrote the manuscript with contributions from all authors.

DECLARATION OF INTERESTS

The authors declare no competing interests.

Received: September 27, 2017
Revised: December 6, 2017
Accepted: February 7, 2018
Published: March 15, 2018

REFERENCES

Arunrattanamook, N., and Marsh, E.N.G. (2017). Kinetic characterization of prenyl-flavin synthase from *Saccharomyces cerevisiae*. Biochemistry. https://doi.org/10.1021/acs.biochem.1027b01131.

Baba, T., Ara, T., Hasegawa, M., Takai, Y., Okumura, Y., Baba, M., Datsenko, K.A., Tomita, M., Wanner, B.L., and Mori, H. (2006). Construction of *Escherichia coli* K-12 in-frame, single-gene knockout mutants: the Keio collection. Mol. Syst. Biol. *2*, 2006.0008.

Baykov, A., Evtushenko, O., and Avaeva, S. (1988). A malachite green procedure for orthophosphate determination and its use in alkaline phosphatase-based enzyme immunoassay. Anal. Biochem. *171*, 266–270.

Chen, H., Manouilov, K., Chu, C., Schinazi, R., McClure, H., and Boudinot, F. (1997). High-performance liquid chromatographic determination of (−)-β-d-2-aminopurine dioxolane and (−)-β-d-2-amino-6-chloropurine dioxolane, and their metabolite (−)-β-d-dioxolane guanine in monkey serum, urine and cerebrospinal fluid. J. Chromatogr. B Biomed. Sci. Appl. *691*, 425–432.

Cox, G.B., Young, I.G., McCann, L.M., and Gibson, F. (1969). Biosynthesis of ubiquinone in *Escherichia coli* K-12: location of genes affecting the metabolism of 3-octaprenyl-4-hydroxybenzoic acid and 2-octaprenylphenol. J. Bacteriol. *99*, 450–458.

Datsenko, K.A., and Wanner, B.L. (2000). One-step inactivation of chromosomal genes in *Escherichia coli* K-12 using PCR products. Proc. Natl. Acad. Sci. USA *97*, 6640–6645.

Dunn, C.A., O'Handley, S.F., Frick, D.N., and Bessman, M.J. (1999). Studies on the ADP-ribose pyrophosphatase subfamily of the nudix hydrolases and tentative identification of trgB, a gene associated with tellurite resistance. J. Biol. Chem. *274*, 32318–32324.

Dyguda-Kazimierowicz, E., Sokalski, W.A., and Leszczyński, J. (2007). Non-empirical study of the phosphorylation reaction catalyzed by 4-methyl-5-β-hydroxyethylthiazole kinase: relevance of the theory of intermolecular interactions. J. Mol. Model. *13*, 839–849.

Ferguson, K.L., Arunrattanamook, N., and Marsh, E.N.G. (2016). Mechanism of the novel prenylated flavin-containing enzyme ferulic acid decarboxylase probed by isotope effects and linear free-energy relationships. Biochemistry *55*, 2857–2863.

Ferguson, K.L., Eschweiler, J.D., Ruotolo, B.T., and Marsh, E.N.G. (2017). Evidence for a 1, 3-dipolar cyclo-addition mechanism in the decarboxylation of phenylacrylic acids catalyzed by ferulic acid decarboxylase. J. Am. Chem. Soc. *139*, 10972–10975.

Gulmezian, M., Hyman, K.R., Marbois, B.N., Clarke, C.F., and Javor, G.T. (2007). The role of UbiX in *Escherichia coli* coenzyme Q biosynthesis. Arch. Biochem. Biophys. *467*, 144–153.

Haas, E. (1938). Isolierung eines neuen gelben ferments. Biochem. Z. *298*, 378–390.

Huo, X., and Viola, R.E. (1996). Functional group characterization of homoserine kinase from *Escherichia coli*. Arch. Biochem. Biophys. *330*, 373–379.

Jacewicz, A., Izumi, A., Brunner, K., Schnell, R., and Schneider, G. (2013). Structural insights into the UbiD protein family from the crystal structure of PA0254 from *Pseudomonas aeruginosa*. PLoS One *8*, e63161.

Kitagawa, M., Ara, T., Arifuzzaman, M., Ioka-Nakamichi, T., Inamoto, E., Toyonaga, H., and Mori, H. (2006). Complete set of ORF clones of *Escherichia coli* ASKA library (a complete set of *E. coli* K-12 ORF archive): unique resources for biological research. DNA Res. *12*, 291–299.

Kopec, J., Schnell, R., and Schneider, G. (2011). Structure of PA4019, a putative aromatic acid decarboxylase from *Pseudomonas aeruginosa*. Acta Crystallogr. Sect. F Struct. Biol. Cryst. Commun. *67*, 1184–1188.

Kuraku, S., Zmasek, C.M., Nishimura, O., and Katoh, K. (2013). aLeaves facilitates on-demand exploration of metazoan gene family trees on MAFFT sequence alignment server with enhanced interactivity. Nucleic Acids Res. *41*, W22–W28.

Kuznetsova, E., Proudfoot, M., Gonzalez, C.F., Brown, G., Omelchenko, M.V., Borozan, I., Carmel, L., Wolf, Y.I., Mori, H., and Savchenko, A.V. (2006). Genome-wide analysis of substrate specificities of the *Escherichia coli* haloacid dehalogenase-like phosphatase family. J. Biol. Chem. *281*, 36149–36161.

Lange, B.M., and Croteau, R. (1999). Isopentenyl diphosphate biosynthesis via a mevalonate-independent pathway: isopentenyl monophosphate kinase catalyzes the terminal enzymatic step. Proc. Natl. Acad. Sci. USA *96*, 13714–13719.

Langella, O., Valot, B., Balliau, T., Blein-Nicolas, M., Bonhomme, L., and Zivy, M. (2016). X! TandemPipeline: a tool to manage sequence redundancy for protein inference and phosphosite identification. J. Proteome Res. *16*, 494–503.

Lawhorn, B.G., Gerdes, S.Y., and Begley, T.P. (2004). A genetic screen for the identification of thiamin metabolic genes. J. Biol. Chem. *279*, 43555–43559.

Letunic, I., and Bork, P. (2016). Interactive tree of life (iTOL) v3: an online tool for the display and annotation of phylogenetic and other trees. Nucleic Acids Res. *44*, W242–W245.

Leys, D., and Scrutton, N.S. (2016). Sweating the assets of flavin cofactors: new insight of chemical versatility from knowledge of structure and mechanism. Curr. Opin. Struct. Biol. *41*, 19–26.

Lichtenthaler, H.K., Schwender, J., Disch, A., and Rohmer, M. (1997). Biosynthesis of isoprenoids in higher plant chloroplasts proceeds via a mevalonate-independent pathway. FEBS Lett. *400*, 271–274.

Lin, F., Ferguson, K.L., Boyer, D.R., Lin, X.N., and Marsh, E.N. (2015). Isofunctional enzymes PAD1 and UbiX catalyze formation of a novel cofactor required by ferulic acid decarboxylase and 4-hydroxy-3-polyprenylbenzoic acid decarboxylase. ACS Chem. Biol. *10*, 1137–1144.

Marshall, S.A., Fisher, K., Ni Cheallaigh, A., White, M.D., Payne, K.A., Parker, D.A., Rigby, S.E., and Leys, D. (2017). Oxidative maturation and structural characterization of prenylated-FMN binding by UbiD, a decarboxylase involved in bacterial ubiquinone biosynthesis. J. Biol. Chem. *292*, 4623–4637.

Meganathan, R. (2001). Ubiquinone biosynthesis in microorganisms. FEMS Microbiol. Lett. *203*, 131–139.

Mizote, T., and Nakayama, H. (1989). The thiM locus and its relation to phosphorylation of hydroxyethylthiazole in *Escherichia coli*. J. Bacteriol. *171*, 3228–3232.

Payer, S., Marshall, S.A., Bärland, N., Sheng, X., Reiter, T., Dordic, A., Steinkellner, G., Wuensch, C., Kaltwasser, S., and Fisher, K. (2017). Regioselective para-carboxylation of catechols by a prenylated flavin dependent decarboxylase. Angew. Chem. Int. Ed. https://doi.org/10.1002/anie.201708091.

Payne, K.A., White, M.D., Fisher, K., Khara, B., Bailey, S.S., Parker, D., Rattray, N.J., Trivedi, D.K., Goodacre, R., Beveridge, R., et al. (2015). New cofactor supports alpha,beta-unsaturated acid decarboxylation via 1,3-dipolar cycloaddition. Nature *522*, 497–501.

Piano, V., Palfey, B.A., and Mattevi, A. (2017). Flavins as covalent catalysts: new mechanisms emerge. Trends Biochem. Sci. *42*, 457–469.

Price, M.N., Dehal, P.S., and Arkin, A.P. (2009). FastTree: computing large minimum evolution trees with profiles instead of a distance matrix. Mol. Biol. Evol. *26*, 1641–1650.

Rangarajan, E.S., Li, Y., Iannuzzi, P., Tocilj, A., Hung, L.W., Matte, A., and Cygler, M. (2004). Crystal structure of a dodecameric FMN-dependent UbiX-like decarboxylase (Pad1) from *Escherichia coli* O157: H7. Protein Sci. *13*, 3006–3016.

Schäfer, M., Drayß, M., Springer, A., Zacharias, P., and Meerholz, K. (2007). Radical cations in electrospray mass spectrometry: formation of Open-Shell species, examination of the fragmentation behaviour in ESI-MS^n and reaction mechanism studies by detection of transient radical cations. Eur. J. Org. Chem. *2007*, 5162–5174.

Shevchenko, A., Tomas, H., Havlis, J., Olsen, J.V., and Mann, M. (2006). In-gel digestion for mass spectrometric characterization of proteins and proteomes. Nat. Protoc. *1*, 2856–2860.

Sobrado, P. (2012). Noncanonical reactions of flavoenzymes. Int. J. Mol. Sci. *13*, 14219–14242.

Teufel, R., Agarwal, V., and Moore, B.S. (2016). Unusual flavoenzyme catalysis in marine bacteria. Curr. Opin. Chem. Biol. *31*, 31–39.

Tian, G., and Liu, Y. (2017). Mechanistic insights into the catalytic reaction of ferulic acid decarboxylase from *Aspergillus niger*: a QM/MM study. Phys. Chem. Chem. Phys. *19*, 7733–7742.

Walsh, C.T., and Wencewicz, T.A. (2013). Flavoenzymes: versatile catalysts in biosynthetic pathways. Nat. Prod. Rep. *30*, 175–200.

White, M.D., Payne, K.A., Fisher, K., Marshall, S.A., Parker, D., Rattray, N.J., Trivedi, D.K., Goodacre, R., Rigby, S.E., Scrutton, N.S., et al. (2015). UbiX is a flavin prenyltransferase required for bacterial ubiquinone biosynthesis. Nature *522*, 502–506.

Xu, W., Dunn, C.A., O'Handley, S.F., Smith, D.L., and Bessman, M.J. (2006). Three new Nudix hydrolases from *Escherichia coli*. J. Biol. Chem. *281*, 22794–22798.

Zhang, H., and Javor, G.T. (2003). Regulation of the isofunctional genes *ubiD* and *ubiX* of the ubiquinone biosynthetic pathway of *Escherichia coli*. FEMS Microbiol. Lett. *223*, 67–72.

Zheng, Y., Liu, Q., Li, L., Qin, W., Yang, J., Zhang, H., Jiang, X., Cheng, T., Liu, W., Xu, X., et al. (2013). Metabolic engineering of *Escherichia coli* for high-specificity production of isoprenol and prenol as next generation of biofuels. Biotechnol. Biofuels *6*, 57.

STAR★METHODS

KEY RESOURCES TABLE

REAGENT or RESOURCE	SOURCE	IDENTIFIER
Bacterial and Virus Strains		
E. coli strain BL21(DE3) Gold	Agilent	230132
E. coli strain BW25113 Δ*nudF::Kmr*	Keio Collection of single-gene knockouts	CGSC#10302
E. coli strain BW25113 Δ*nudJ::Kmr*	Keio Collection of single-gene knockouts	CGSC#9049
E. coli strain BW25113 Δ*nudJ::Kmr*, Δ*nudF::Cmr*	This study	N/A
E. coli strain BL21(DE3) Δ*thiM::Cmr*	This study	N/A
Chemicals, Peptides, and Recombinant Proteins		
Isopropyl β-D-1-thiogalactopyranoside (IPTG)	Bioshop	Cat#IPT001.100
Dimethyl sulfoxide	Bioshop	Cat#DMS555.500
Riboflavin	Sigma-Aldrich	Cat#R7774
Prenol (3-methyl-2-buten-1-ol)	Sigma-Aldrich	Cat#W364703
Ni-NTA Superflow resin	Qiagen	Cat#30450
Sodium dodecyl sulfate	Bioshop	Cat#SDS001
BugBuster® Protein Extraction Reagent	Novagen	Cat#71456-3
Bradford reagent	BioRad	Cat#5000006
phenylmethylsulfonyl fluoride	Bioshop	Cat#PMS123
4-(2-hydroxyethyl)-1-piperazineethanesulfonic acid (HEPES)	Sigma-Aldrich	Cat#H4034
Sodium Chloride	Bioshop	Cat#SOD001.1
Flavin mononucleotide	Sigma-Aldrich	Cat#R7774
Dimethyl-allyl phosphate (DMAP)	Can Syn Chem Corp	N/A (customized product)
Dimethyl-allyl pyrophosphate (DMAPP)	Sigma	Cat#D4287
Potassium orthophosphate	Bioshop	Cat#PPM302.1
Sodium dithionite	Sigma-Aldrich	Cat#S-1256
Tris-HCl	Sigma-Aldrich	Cat#T1503
LB Broth Miller	BioShop	Cat#LBL407
Terrific Broth	BioShop	Cat#TER409.5
Magnesium chloride	BioShop	Cat#MAG510
adenosine triphosphate	Sigma-Aldrich	Cat#A7699
polyphosphate	Aldrich	Cat#305553
Malachite Green Reagent	Prepared in this study based on (Baykov et al., 1988)	N/A
Nicotinamide adenine dinucleotide, reduced disodium salt hydrate (NADH)	BioShop	Cat#NAD002.1
5-ethynyl-4-methyl-1,3-thiazole	Millipore Sigma	Cat#8.14928.0025
2-(N-Morpholino) ethanesulfonic acid potassium salt (MES)	BioShop	Cat#MES503
Trans-cinnamic acid	Aldrich	Cat#C80857
α-fluorocinnamic acid	Aldrich	Cat#163848
Acetonitrile	Caledon	SKU:1401-7-40
Hydrochloric acid	BioShop	Cat#HCL 666.1
Glycerol	BioShop	Cat#GLY001.4
Bromophenol blue	Fluka	Cat#18040
Dithiothreitol	BioShop	Cat#DTT002

(*Continued on next page*)

Continued

REAGENT or RESOURCE	SOURCE	IDENTIFIER
Coomassie blue	Sigma	Cat#B7920
Trifluoroacetic acid	Sigma	Cat#T6508
Formic acid	Aldrich	Cat#F0507
Ammonium acetate	Fluka	Cat#9689
Methanol	Caledon	SKU:6701-7-40
$prFMN_{radical}$	This study	N/A
$prFMN_{imminium}$	This study	N/A
Lactate dehydrogenase	Sigma	Cat#L3888
Pyruvate kinase	Sigma	Cat#P1506
Critical Commercial Assays		
QuikChange™ site-directed mutagenesis kit	Agilent	Cat#200524
Deposited Data		
A phylogenetic tree of UbiX proteins	This study	http://itol.embl.de/tree/142150588823901497476579
Oligonucleotides		
thiM forward λ–red primer: 5'-ACCGGCAATCGTCAGAGCGTTAATTCGTTTCATGCCTGCACCTCCTGCGTGTGTAGGCTGGAGCTGCTTC-3'	This study	N/A
thiM reverse λ–red primer: 5'ACGGACCACCAGGTCATTGCTTCTTCACGTTATGGCAGGAGCAAACTATGATGGGAATTAGCCATGGTCC-3'	This study	N/A
thiM forward check primer: 5'-GCAATCGTCAGAGCGTTAATTC-3'	This study	N/A
thiM reverse check primer: 5'-CCACCAGGTCATTGCTTCTTC-3'	This study	N/A
nudF forward λ–red primer: 5'-TCAGGAAAGTCAGGTGTGTAACGCTTCATTTATGCCCACTCATTTTTTAAGTGTAGGCTGGAGCTGCTTC-3'	This study	N/A
nudF reverse λ–red primer: 5'-TCGCTGAAATTCACATTTAATTCACTATTAGTGCCAGGACATTAACAATGATGGGAATTAGCCATGGTCC-3'	This study	N/A
nudF forward check primer: 5'-CAATTGTGAAAAGTTCATCTCGC-3'	This study	N/A
nudF reverse check primer 5'-CAATTTAACACATGACTGCTCAAAC-3'	This study	N/A
Recombinant DNA		
Modified pET15b vector	Prof. Cheryl Arrowsmith, University of Toronto	Addgene plasmid #26093
Codon optimized Fdc1 from *Aspergillus niger*	Prof. David Leys, University of Manchester	N/A
Plasmids with modified pET15b vector and ubiX genes listed in Table S2	This study	N/A
ASKA Collection clones	NBRP	ECOLI-4866
KEIO Collection clones	NBRP	ECOLI-4863
Software and Algorithms		
Itol	(Letunic and Bork, 2016)	http://itol.embl.de/
FastTree 2.1.5	(Price et al., 2009)	http://www.microbesonline.org/fasttree/

(*Continued on next page*)

Continued

REAGENT or RESOURCE	SOURCE	IDENTIFIER
MAFFT	(Kuraku et al., 2013)	http://mafft.cbrc.jp/alignment/server/
Geneious 8.1.8	Biomatters	RRID:SCR_005342; www.geneious.com
GraphPad Prism (version 5)	GraphPad software	RRID:SCR_015807; https://www.graphpad.com/scientific-software/prism/

CONTACT FOR REAGENT AND RESOURCE SHARING

Information and request for resources and reagents should be directed and will be fulfilled by the lead contact, Dr. Alexander F. Yakunin (a.iakounine@utoronto.ca).

EXPERIMENTAL MODEL AND SUBJECT DETAILS

All proteins and plasmids used for *in vitro* studies were purified from *Escherichia coli* strain BL21(DE3) Gold as described in the text and the Key Resources Table. The *E. coli* strain BW25113 Δ*nudF::Km*^{r} and Δ*nudJ::Km*^{r} strains were obtained from the Keio Collection of single-gene knockouts (Baba et al., 2006).

Culture Conditions for *E. coli* Strains

All *E. coli* strains used in this study were routinely cultured in LB Broth Miller (BioShop) at 37°C and 200 rpm. The *E. coli* cultures for recombinant protein expression and purification were inoculated to Terrific Broth (1% inoculation) as described in Protein Expression and Purification in Method Details.

METHOD DETAILS

Phylogenetic Analysis

A multiple sequence alignment was generated from 9,043 InterPro family (IPR004507) sequences using online MAFFT alignment tool. The original dataset was reduced to 5,534 sequences using the Max Align and CD HIT refinement strategies from the same website. The phylogenetic tree was constructed with the "approximately maximum-likelihood" algorithm provided by FastTree 2.1.5 built in Geneious 8.1.8. The phylogenetic tree was then visualized using Itol.

Gene Cloning and Mutagenesis

The UbiX genes from different organisms (Table S2) were amplified by PCR from genomic DNA and cloned into a modified pET15b vector (Novagen) containing an N-terminal His_6-tag as described previously (Kuznetsova et al., 2006). Site-directed mutagenesis of the *E. coli* kinase ThiM was performed using the QuikChange™ site-directed mutagenesis kit (Agilent) according to the manufacturer's protocol, and mutations were verified by DNA sequencing. The plasmids were transformed into *E. coli* strain BL21 (DE3) Gold as expression host. The *E. coli* strain BW25113 Δ*nudF::Km*^{r} and Δ*nudJ::Km*^{r} strains were obtained from the Keio Collection of single-gene knockouts (Baba et al., 2006). The one-step gene inactivation method of Datsenko and Wanner (Datsenko and Wanner, 2000) was used to create a double Δ*nudJ::Km*^{r}, Δ*nudF::Cm*^{r} knockout strain (in BW25113) and a *thiM* deletion strain (Δ*thiM::Cm*^{r}; in BL21(DE3) Gold)). The primer sequences are available in Key Resources Table.

Protein Expression and Purification

For recombinant expression and purification of UbiX-like proteins, the cultures were grown under aerobic conditions at 37 °C in a shaker using Terrific Broth (200 rpm) to the optical density ($OD_{600\ nm}$) 0.8-1 followed by induction with 0.4 mM isopropyl β-D-1-thiogalactopyranoside (IPTG) and overnight incubation at 16 °C (for aerobic protein expression). For anaerobic protein expression, after the IPTG induction the cultures were transferred to screw-capped glass bottles and supplemented with Dimethyl sulfoxide (2 mL/L) and (if indicated) riboflavin (0.2 mM) and/or prenol (1 mM), and incubated overnight at room temperature with constant stirring. Recombinant proteins were purified to at least 95% homogeneity using metal-chelate affinity chromatography on Ni-NTA Superflow resin as previously described (Kuznetsova et al., 2006), and protein purity was analyzed by SDS-PAGE (Figure S2). The *E. coli* kinases and phosphohydrolases (Nudix) were expressed using the ASKA Collection clones for expression of *E. coli* proteins (Kitagawa et al., 2006) and affinity purification according to the manufacturer's protocol. In brief, cells were collected by centrifugation at 9,000 × g for 20 min, suspended in HEPES buffer (50 mM HEPES, 300 mM NaCl and 10 mM imidazole, pH 7.5), and sonicated in an ice bath for 45 min (3 s on and 4 s off). The lysate was centrifuged at 38,000 × g for 20 min and the supernatant was passed through a glass column containing about 0.5 mL Ni-NTA resin (Qiagen). After washing with HEPES buffer (20 mM imidazole), proteins were eluted with 5–7 mL of HEPES buffer containing 250 mM imidazole and 5% (w/v) glycerol. The protein stock solutions were frozen in liquid nitrogen and stored at −80 °C. The N-terminal hexa-histidine tag was retained for all experiments.

Enzyme Assays

The *E. coli* strain BL21(DE3) cell lysates for enzyme assays and proteomics analysis were prepared using the BugBuster® Protein Extraction Reagent according to manufacturer's protocol (except that 1 mM phenylmethylsulfonyl fluoride was added to the cell suspension for protease inhibition). Purified proteins were at least 95 % pure based on SDS-PAGE analysis (Figure S2). Anaerobic assays were performed in an anaerobic glove box (Coy) with an atmosphere of 10% CO_2, 10% H_2, and balancing N_2.

In Vitro FMN Prenylation by Purified UbiX

The reaction mixtures (110 μL) contained 40 mM HEPES-Na buffer (pH 7.5), 0.4 M NaCl, 60 μM FMN, 0.1 mM dimethyl-allyl monophosphate (DMAP), 20 mM K-orthophosphate, and up to 5 mg of cofactor-free (colorless) AF1214. Under anaerobic conditions (in a glove box), the reaction mixture was reduced by the addition of 3 mM sodium dithionite (DT; 2 h under anaerobic conditions at 37 °C), filtered through 3 kDa spin filters, oxidized on air (10-20 min), and the flow-through fraction was used for absorption spectra analysis. Anaerobic reaction mixtures for DMAP saturation experiments with the $AF1214^{FMN}$ (yellow) contained 100 mM HEPES-Na (pH 7.5), 0.4 M NaCl, 3 mM DT, 0-0.175 mM DMAP, and 0.175 mM $AF1214^{FMN}$. After 1 h incubation at 37 °C, the reaction mixtures were oxidized on air for 10 min followed by absorbance analysis at 550 nm. All enzyme assays were conducted in duplicates or triplicates as indicated on figures.

UbiX-based Prenol Kinase Screens

The colorimetric prenol kinase screen is based on the ability of AF1214 to prenylate reduced FMN using DMAP and retain the oxidized prFMN after the reaction producing a purple-colored protein containing $prFMN_{radical}$ with the λ_2 at 550 nm. The screen includes two steps: prenol phosphorylation to DMAP and FMN prenylation. The prenol phosphorylation reaction mixture (0.1 mL) contained 100 mM HEPES-Na buffer (pH 7.5), 0.3 M NaCl, 10 mM $MgCl_2$, ATP (10 mM for cell lysates and 5 mM for purified proteins), 1 mM polyphosphate, prenol (10 mM for cell lysates and 5 mM for purified proteins), 10 mg/mL cell lysate or 0.1 mg/mL purified protein was incubated for 1 h at 37°C with shaking at 200 rpm. After 1 h incubation at 37°C, the reaction mixtures were supplemented with 0.1-0.3 mg of the reduced (with 3 mM DT) $AF1214^{FMN}$, followed by 1 h incubation at 37°C in an anaerobic glove box. Finally, the reaction mixtures containing $AF1214^{prFMNred}$ were oxidized on air, and the absorbance at 460 nm (λ_2 for $UbiX^{FMN}$) and 550 nm (λ_2 for $UbiX^{prFMNradical}$) were recorded. The ($\lambda_{550\ nm}$ /$\lambda_{460\ nm}$) ×10 values higher than 0.2 or formation of a purple-colored solution were considered as positive results for the presence of prenol kinase activity. The determination of the DMAP product in cell lysate assays was carried out using LC-MS as described in the MS analysis section.

DMAPP Dephosphorylation Activity

Assays were performed in 96-well microplates using reaction mixtures (25 μL) containing 100 mM Tris-HCl (pH 8.0; for assays with purified phosphohydrolases) or 100 mM HEPES-Na (pH 7.0; for assays with cell lysates), 0.1-1 mM dimethyl-allyl pyrophosphate (DMAPP), 5 mM $MgCl_2$, 0.5 mM $MnCl_2$, and purified phosphohydrolases (2-10 μg) or cell lysates (25 μg). After 10-20 min incubation at 37 °C, the reaction was stopped by the addition of Malachite Green reagent and the production of orthophosphate was measured based on absorbance at 630 nm (Baykov et al., 1988). The determination of the DMAP product and residual amounts of DMAPP in cell lysate assays was carried out using LC-MS as described in the MS analysis section.

Prenol and Thiazole Phosphorylation Assays

Kinase activities of purified ThiM were assayed spectrophotometrically at 37 °C using a microplate-based enzyme-coupled assay with lactate dehydrogenase and pyruvate kinase as previously described (Huo and Viola, 1996). Reaction mixtures (0.2 mL) contained 100 mM HEPES-Na (pH 7.5), 10 mM $MgCl_2$, 5 mM phosphoenolpyruvate, 0.3 mM NADH, 2 mM ATP, lactate dehydrogenase (2.5 units), pyruvate kinase (1.9 units), 5-ethynyl-4-methyl-1,3-thiazole or prenol as substrate (1-50 mM), and purified protein (5-10 μg). In addition, the kinase reaction product ADP was analyzed using reversed phase chromatography on a Varian ProStar HPLC system equipped with a AXXI-CHROM ODS column (5-μm-size particles, 4.6 × 250 mm; Cole Scientific) (Chen et al., 1997).

Fdc1 Activation and Decarboxylation Assays

For activation of the purified *A. niger* apo-Fdc1, the reaction mixture (17 μL) containing 100 mM Na-phosphate buffer (pH 6.0), 200 mM NaCl, 0.25 nmol of $PA4019^{prFMN}$ (or $AF1214^{prFMN}$, or equimolar amounts of free prFMN forms) was incubated with apo-Fdc1 (0.25 nmol) for 5-60 min under aerobic or anaerobic conditions at room temperature. For Fdc1 activation experiments with orthophosphate saturation, the reaction mixture contained 100 mM MES-K buffer (pH 6.0) and 0-10 mM phosphate. The decarboxylation activity of activated Fdc1 was determined by following the consumption of substrates spectrophotometrically as previously described (Payne et al., 2015). In brief, the reaction mixture (0.2 mL) containing 100 mM MES-K buffer (pH 6.0), 200 mM NaCl, 0.2 mM $MnCl_2$, 0.3 mM substrate (cinnamic acid or α-fluorocinnamic acid), and 1 μg of Fdc1 were incubated in a 96-well plate (Corning) at 30°C for 20-40 min with a read in every 30 s in a SpectraMax UV-vis spectrophotometer (Molecular Devices). The rate of cinnamic acid and α-fluorocinnamic acid consumption was monitored at $\lambda_{270\ nm}$ and $\lambda_{265\ nm}$, respectively.

Extraction of prFMN

Purified UbiX-like proteins (AF1214 or PA4019) were saturated with prFMN *in vitro* by incubating in a reaction mixture containing 100 mM Na-phosphate buffer (pH 7.0), FMN (0.1-1 mM), and DMAP (1 mM) under anaerobic conditions. After reduction with DT (3 mM, 37°C, 1 h), the proteins were oxidized by air (producing $prFMN_{radical}$), precipitated with ice-cold 50 % (v/v) acetonitrile and washed two times with the same solution. All further purification steps were performed in an anaerobic chamber (Coy) using anaerobic solutions. For the purification of free $prFMN_{radical}$ (Structure B, Figure 4) from PA4019, the protein was resuspended in 70% acetonitrile and heated for 10 min at 80°C on a shaker (800 rpm). For protonated $prFMN_{radical}$ (form C in **Main Text** Figure 4) purification, UbiX-like proteins ($AF1214^{prFMN}$ or $PA4019^{prFMN}$) were resuspended in 50 % acetonitrile and acidified with 50-100 mM HCl. The proteins were precipitated by the addition of acetonitrile to a final concentration of 86 % and centrifuged at 13,000 x g for 10 min at room temperature. The solution was either directly used for assays or concentrated using a rotary evaporator until full acetonitrile evaporation. Cofactor preparations were stored frozen in the O-ring-capped plastic tubes at -80 °C.

Determination of prFMN Extinction Coefficient

For the determination of extinction coefficient of free protonated $prFMN_{radical}$ (C), we used the purified AF1214 saturated with FMN. One half of this sample was used to extract FMN (in triplicate) and determine its concentration using a calibration curve generated with synthetic FMN and extinction coefficient (10.9 mM^{-1} cm^{-1}, $\lambda_{442\ nm}$). The other half was incubated anaerobically with an excess (6x) of DMAP for the complete transformation of FMN to prFMN and subsequent cofactor extraction (also in triplicate). LC-MS analysis of the $AF1214^{FMN}$ extracts and $AF1214^{prFMN}$ extracts revealed negligible amounts of FMN and riboflavin, respectively, suggesting complete transformation of FMN to prFMN. Thus, we assume that the concentration of FMN in the $AF1214^{FMN}$ extract is equal to that of protonated $prFMN_{radical}$ in the $AF1214^{prFMN}$ extract. Using serial dilutions of purified protonated $prFMN_{radical}$ and its λ_2 at 490 nm, we established a calibration curve and determined the extinction coefficient of prFMN to be 6.3 mM^{-1} cm^{-1} ($\lambda_{490\ nm}$).

Mass Spectrometry

For protein mass spectrometry, the *E. coli* BL21 (DE3) wild-type and Δ*thiM* mutant strains grown without or with the addition of 1 mM prenol were used. The strains were grown in duplicate at 37 °C on terrific broth to OD_{600nm} 0.6-0.8, and then incubated overnight at 16 °C. The cells were collected by centrifugation at 10,000 x g for 10 min and lysed using BugBuster Master Mix as described in manufacturer's protocol. The lysates were mixed with 2 times SDS loading buffer (50 mM Tris-HCl (pH 6.8), 10 % SDS, 40 % glycerol, 3 mM bromophenol blue, 0.5 M DTT, separated on 15 % SDS-PAGE gels, stained by Coomassie Blue for 2 h and de-stained overnight. The portion of the gel corresponding to molecular mass 10-35 kDa was excised and used for overnight trypsin digestion as described previously (Shevchenko et al., 2006). Trypsin digestion was stopped using 0.1 % TFA and desalted using C-18 OMIX tips (Agilent) according to the manufacturer's instructions. Protein samples were resuspended in 0.1 % formic acid and analyzed by mass spectrometry using a Q Exactive MS system (Thermo Scientific) at the BioZone Mass Spectrometry Facility (University of 663 Toronto, Toronto, Canada; https://www.biozone.utoronto.ca/mass_spec/). Raw MS data was processed and analyzed using X!TandemPipeline (Langella et al., 2016) and is presented in Table S4 (in a separate Excel spreadsheet).

The LC-MS platform for small molecule analysis contained a Dionex Ultimate 3000 UHPLC system equipped with a photodiode array detector and a Q-Exactive MS equipped with a HESI II source (all from Thermo Scientific). Control of the system and data handling was performed using Thermo XCalibur 2.2 software and Chromeleon 7.2 software. Separation by liquid chromatography was conducted at 40°C on a Thermo Hypersil Gold C18 column (50 mm x 2.1 mm, 1.9 μm particle size, Thermo Scientific). The pump was run at a flow rate of 0.2 mL/min. Solvent A was water containing 5 mM ammonium acetate (pH 6.0); solvent B was methanol containing 5 mM ammonium acetate (pH 6.0). For prFMN and FMN analysis, the gradient was 0-1 min, 2 % B; 1-7 min, linear increase to 90 % B; 7-10.5 min, hold at 90% B; 10.5-11 min, return to initial conditions (2 % B) and hold for 7 mins prior to next sample. For DMAP and DMAPP analysis, the gradient was 0 min, 2 % B; 0-1 min, 2 % B; 1-4 min, 90 % B; 4-7 min, 90 % B; 7-7.5 min, return to initial conditions (2 % B) and hold for 4.5 mins prior to next sample. The autosampler temperature was maintained at 10°C and the injection volume was 20 μL. Data collection was done in both positive and negative ionization modes with a scan range of m/z 200-700, and mass resolution of 140,000, Automatic Gain Control target of 3e6 and a maximum injection time of 200 ms.

QUANTIFICATION AND STATISTICAL ANALYSIS

Enzyme kinetics data were analyzed in GraphPad Prism using in-built algorithms. Kinetic parameters were calculated by nonlinear regression analysis of raw data to fit to the Michaelis-Menten function using GraphPad Prism Software (version 5 for Windows, GraphPad Software, San Diego, CA). Means and standard deviations have been derived from the best fit of the data, or based on two or three independent measurements, as specified in the figures or tables, unless noted otherwise.

DATA AND SOFTWARE AVAILABILITY

The phylogenetic tree of 5,534 unique UbiX proteins can be accessed through Itol website (http://itol.embl.de/tree/14215058882390149747657 9). All other data supporting the findings of this study are available within the paper and its Supplemental Information files.

Deposited Data

The NBRC0004 protein sequence reported in this paper is: MKKLVVGISGATGAIYGIRLLEVLRELEVETHLVVSEGAARTIRMETQYEFSEVTKLATHVYDIKNVGASIASGSFPIDGMAIVPCSIKSLSALANSYNDNLLIRAADVNLKEKRKVVVMVRETPLHGHLRLMMQVAEAGGVILPPMPAFYHQPRSLQEIIDQTIGKVLDQFGLDGKLFSRWEGSGILRSVSKKSI.